ARMY RESEARCH LABORATORY

Electrical Exploding Nickel and Tungsten Wires in Air and Water

by G. B. Vunni

ARL-CR-619 **February 2009**

prepared by

Oak Ridge Institute for Science and Education
P.O. Box 117
Oak Ridge, TN 37821-0017

under contract

W911QX04C0129

NOTICES

Disclaimers

The findings in this report are not to be construed as an official Department of the Army position unless so designated by other authorized documents.

Citation of manufacturer's or trade names does not constitute an official endorsement or approval of the use thereof.

Destroy this report when it is no longer needed. Do not return it to the originator.

Army Research Laboratory
Aberdeen Proving Ground, MD 21005-5066

ARL-CR-619 **February 2009**

Electrical Exploding Nickel and Tungsten Wires in Air and Water

G. B. Vunni

prepared by

Oak Ridge Institute for Science and Education
P.O. Box 117
Oak Ridge, TN 37821-0017

under contract

W911QX04C0129

REPORT DOCUMENTATION PAGE	Form Approved OMB No. 0704-0188

1. REPORT DATE *(DD-MM-YYYY)*	2. REPORT TYPE	3. DATES COVERED (From - To)
February 2009	Final	September 2008–September 2009

4. TITLE AND SUBTITLE
Electrical Exploding Nickel and Tungsten Wires in Air and Water

5a. CONTRACT NUMBER
W911QX04C0129

5b. GRANT NUMBER

5c. PROGRAM ELEMENT NUMBER

6. AUTHOR(S)
G. B. Vunni

5d. PROJECT NUMBER
611102H43000

5e. TASK NUMBER

5f. WORK UNIT NUMBER

7. PERFORMING ORGANIZATION NAME(S) AND ADDRESS(ES)
Oak Ridge Institute for Science and Education
P.O. Box 117
Oak Ridge, TN 37821-0017

8. PERFORMING ORGANIZATION REPORT NUMBER

9. SPONSORING/MONITORING AGENCY NAME(S) AND ADDRESS(ES)
U.S. Army Research Laboratory
ATTN: AMSRD-ARL-WM-TE
Aberdeen Proving Ground, MD 21005-5066

10. SPONSOR/MONITOR'S ACRONYM(S)

11. SPONSOR/MONITOR'S REPORT NUMBER(S)
ARL-CR-619

12. DISTRIBUTION/AVAILABILITY STATEMENT
Approved for public release; distribution is unlimited.

13. SUPPLEMENTARY NOTES

14. ABSTRACT

Nickel wire of diameter d = 230 μm and tungsten wire of diameter d = 150 μm were exploded in air and water. Plasmas were formed by rapid electrical discharge through thin wires in air and immersed in a water bath. Energy deposited into the wires at different stages of heating in air and water was estimated from the experiments. It was shown that ~30% more energy was deposited in water than in air.

15. SUBJECT TERMS
plasma, electrical conductivity, copper, energy, temperature

16. SECURITY CLASSIFICATION OF:			17. LIMITATION OF ABSTRACT	18. NUMBER OF PAGES	19a. NAME OF RESPONSIBLE PERSON
a. REPORT	b. ABSTRACT	c. THIS PAGE			George B. Vunni
UNCLASSIFIED	UNCLASSIFIED	UNCLASSIFIED	UL	22	19b. TELEPHONE NUMBER (*Include area code*) 410-278-3748

Standard Form 298 (Rev. 8/98)
Prescribed by ANSI Std. Z39.18

Contents

List of Figures

List of Tables

Acknowledgments

The authors wish to acknowledge Dr. Charles Hummer of the U.S. Army Research Laboratory (ARL) and Prof. Alan DeSilva of the University of Maryland College Park for helpful discussions on pulse power, plasma physics, wire explosion, and novel techniques of plasma diagnostics. We would like to thank Dr. John Powell of ARL for reviewing this work and Keith Mahan of ARL for helping with the experimental work. This research was supported, in part, by funding from ORISE for postdoctoral research at ARL, Aberdeen Proving Ground, MD, under contract number W911QX04C0129.

INTENTIONALLY LEFT BLANK.

1. Introduction

In a number of papers, attempts were made to study the influence of a surrounding medium on the energy deposited during electrical wire explosions (*1–4*). A recent report by Sarkisov et al. (*3*) on the electrical explosion of titanium wires showed that the energy deposited into the wire doubled for explosions in air when compared to that deposited for explosions in vacuum. In a similar experiment, Bennett (*5*) showed that surface impurities (such as absorbed gases and hydrocarbons) played an important role in energy deposition during electrical explosion and vaporizing impurities formed a plasma shell around the exploding wire. The plasma shell forces the current away from the wire core and reduces joule energy deposition. On the other hand, Grinenko et al. (*4*) reported that the plasma shell was significantly reduced for wires exploded in water, resulting in significant energy deposition. Clearly, to improve energy deposition, it is necessary to minimize current diversion from the wire core to the plasma shell during wire explosion. One possible way to solve this problem is to explode wires in water or air.

To obtain data suitable for electrical measurements, we created a cylindrical plasma by vaporizing a metal wire with a burst of current in air and in water following the experimental techniques advanced previously by DeSilva and Kunze (*6*) and DeSilva and Katsouros (*7*). The resulting plasma column expanded radially, compressing the surrounding water or air and causing a cylindrical shock wave to move radially outward. The plasma remained quite stable during this expansion in water, and very little diffusion of energy occurred between the plasma and water on the short time scale of the observation. In our experiment, the plasma was assumed to be uniform within the plasma water boundary. However, in air, the plasma had a zero pressure outer boundary and was certainly not uniform over the cross section.

The aim of this report is to investigate plasma dynamics associated with exploding nickel and tungsten wires and to provide experimental data for verification and validation of the ALEGRA (Arbitrary Lagrangian Eulerian General Research Application) code. Knowledge of some of the material properties at high temperature and pressures (plasma state) is extremely important for several U.S. Army-related applications, such as electromagnetic armor, electrical conduction in shaped charge jets, and electromagnetic propulsion.

2. Experimental Procedure

Figure 1 shows a schematic diagram of the discharge chamber. It consists of an aluminum cylinder 45 cm in diameter and 25 cm in height. Current was introduced coaxially from the bottom electrode, and the load wire was stretched between this electrode and a grounded support positioned 54 mm above the electrode.

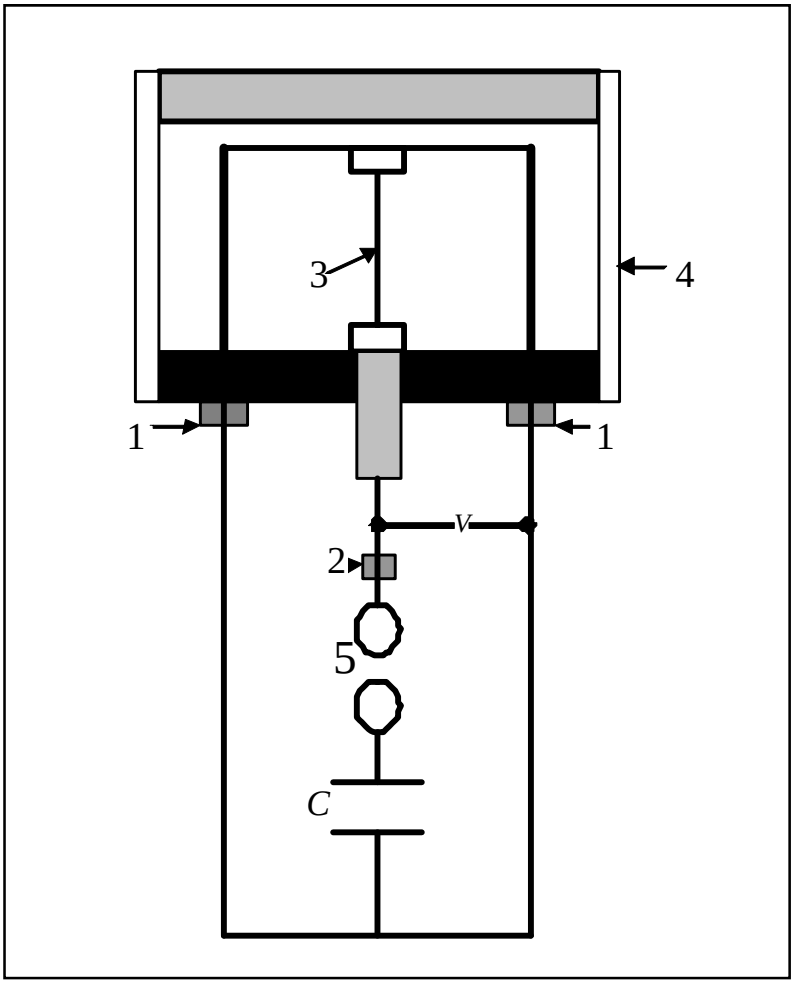

Figure 1. Schematic diagram of experimental configuration for voltage and current measurements: (1) Rogowski coil, (2) Pearson coil, (3) wire, (4) discharge chamber used to hold water, (S) spark gap, (C) capacitor, and (V) voltage divider. The capacitor charging unit and electrical control are not shown.

Current return from the top of the wire took place through four rods positioned symmetrically about the wire. The chamber was fitted with four windows, placed 90° apart, to allow optical observation of the plasma. After a load wire was installed, the chamber was filled with deionized water (for experiments conducted in water). Current was driven from a single capacitor of 256 μF rated at 10 kV (they have been used in this work only up to about 4 kV) and switched by a vacuum sparkgap. A Pearson coil was used to measure the current, and a Rogowski coil with a sensitivity of 31.8 A/μs was used to measure the current time derivative. A capacitive voltage divider (1000:1 ratio) was used to measure the voltage at the load. The signals from the Rogowski and Pearson coil were recorded using a four-channel DSO6104A Agilent oscilloscope.

The inductance of the circuit, exclusive of the wire load, was about 505 nH. This circuit inductance was measured by installing a cylindrical plug in place of the wire load and firing. Such a load was purely inductive. It was from the observed ringing period that the bank inductance was determined. Voltage and current were recorded for this inductive load, and subsequent comparison of *V(t)* with $\frac{dI(t)}{dt}$ served to confirm that the diagnostics were functioning correctly. From the ratio of these quantities, the overall circuit inductance was determined.

3. Analysis

In interpreting the data, we assumed uniformity of the plasma column and homogeneous heating of the wires. In our experiments, we neglected radial inhomogeneity of the current due to skin effect because of the small wire diameter. We also expected no effect from magnetic diffusion time τ in the final measurements. This diffusion time τ was estimated from the general solution of the differential equation for the magnetic field diffusion into an infinitely long rod. This general solution was a sum of terms with decreasing time scales. The characteristic time for magnetic diffusion in microseconds is approximately $\tau = \frac{2170\ r_0^{\,2}}{\rho}$, where ρ is the resistivity in μΩ-cm, r_0 is the radius of the wire in centimeters, and the factor 2170 has accounted for the 10^{-6} in the denominator (*8*). For nickel (*9*) wire with resistivity $\rho(1728\,K) \sim 60\mu\Omega - cm$, $r \sim 115\mu m$, 1.15×10^{-2} cm, and the diffusion time is approximately 4.8 ns, which is far less than the current rise time of ~1.3 μs. T hus, there is a enough time for the field to penetrate the wire, and our assumption of homogeneity in the heating of the wire is valid.

In our experiment, we recorded $\frac{dI}{dt}$ (the time derivative of the current) from the Rogowski coil and the voltage across the plasma. The current was obtained by either numerically integrating $\frac{dI}{dt}$ or directly from the Pearson coil. We confirmed that the two methods gave similar results.
The recorded voltage is given as

$$V(t) = IR + L_w \frac{dI}{dt} + I\frac{dL_w}{dt}\ , \qquad (1)$$

where I is the current through the wire, R is the resistance of the wire, and L_w is the inductance of the wire. The contributions represented by the last two terms on the right must be subtracted out in order to obtain the true ohmic potential $V_R = IR$ across the wire. R is then the ratio V_R / I.

As the $L_w\, dI/dt$ and IdL_w/dt terms are time dependent, we analyzed the data for each 2-ns time step. The energy input to the wire was calculated by integrating the product of the current and voltage $E(t) = \int_0^t I(t)V_R(t)dt$, where V_R is the measured voltage less the $L_w \frac{dI}{dt} + I\frac{dL_w}{dt}$ contributions. The wire inductance L_w was determined as the ratio of measured voltage to the current time derivative ($\frac{V(t)}{dI/dt}$), since for the first few microseconds, the resistance of the wire and dL_w/dt are both small enough that the IR and IdL_w/dt terms are negligible relative to the $L_w\, dI/dt$ term. This procedure checks well with the wire inductance ($L_{Ni} = 60nH$ and $L_W = 70nH$) computed using the formula given in reference (*10*).

To make a reasonable estimate of the energy input, we compared the experimental energy input derived by integrating the current and voltage with energy derived from the thermodynamic relationship given by the following:

$$E_v = m(c_s \Delta T + L_f + c_l \Delta T_v + L_v)\ , \tag{2}$$

where m is the mass of the wire, c_s is the specific heat at room temperature, c_l is the specific heat at the melting temperature (*11*), ΔT is the change in temperature from room temperature to melting temperature, $\Delta T_v = T_b - T_m$ is the change in temperature from the melting point to the vaporization point, and L_f and L_v are the latent heats of fusion and vaporization. A summary of the thermophysical properties of pure nickel and tungsten wire is shown in table 1. In reality, the exploded wires are alloys that may have slightly different specific heats, latent heats, and melting and boiling temperatures.

4. Results and Discussion

4.1 Nickel

Figures 2a and c show the current, voltage, and deposited energy waveforms for nickel wire explosions in air and water.

As the wire was heated in air (figure 2a), the current rose rapidly to a maximum value of about 4.7 kA in 1.5 μs, then dropped to nearly 0. The current through the wire was approximately constant in the 2.5–5.5-μs range, which implied that the resistivity was nearly constant in this region. This time region probably corresponded to the latent heat of vaporization, where energy was added to the wire without any change of temperature. At about 6 μs, the wire became extremely nonconducting. Presumably, at this time, the wire exploded.

Table 1. Thermodynamic properties of nickel and tungsten wires.

Properties	***Ni***	***W***
$T_m(K)$	1728	3695
$T_v(K)$	3110	5828
$d(cm)$	0.023	0.0150
$l(cm)$	5.4	5.4
$m(g)$	0.020	0.018
$c_s(J/g.K)$	0.444	0.136
$c_l(J/g.K)$	0.645	0.262
$L_f(J/g)$	300.0	192.0
$L_v(J/g)$	6457.0	2296.0
$E_m(J)$	12.7	8.1
$E_{Tm}(J)$	18.5	11.5
$E_v(J)$	36.5	22.0
$E_{Tv}(J)$	165.0	64.0

Notes: T_m and T_v = melting and vaporization temperature; d and l = diameter and length of the wires; m = mass, c_s and c_l = solid and liquid specific heat capacity, L_f; $E_m(J)$ = latent heat of fusion and vaporization; $E_m(J)$ = the energy required to bring the wire to the melting point; $E_{Tm}(J)$ = total energy required to melt the wire; $E_v(J)$ = energy required for onset of vaporization; and $E_{Tv}(J)$ = total energy to vaporize the wire.

Meanwhile, the voltage rose with various changes in slope to a maximum value of about 4.7 kV. The voltage plot revealed some interesting features, and the characteristic points were marked χ, α, β, γ, and δ (see figure 2). At χ (manifested by a small inflection in the voltage), ~2.6 J of energy was deposited in the wire. This energy was sufficient to raise the temperature of the nickel wire to the Curie temperature (631 K). Beyond χ, the voltage rose to a small peak at α, where 12.4 J of additional energy was deposited into the wire, sufficient to raise the temperature of the wire to 1728 K (melting point). After α, an additional 6 J of energy equal to the heat of fusion was added to melt the wire at β. Meanwhile, at γ, ~35 J of energy was deposited into the wire, sufficient for onset of vaporization. We associated the voltage spike at label δ to arcing in the plasma.

The resistance, plotted together with the energy deposited in air, is shown in figure 2b. Indicated on the plot are the corresponding transitions labeled χ, α, β, γ, and δ. The resistance was determined from the measured current and voltage. The initial resistance was about 0.1 Ω. The resistance then increased with heating to 1.35 Ω at about 3.5 μs. A roughly constant resistance phase followed for about 2 μs, and then the resistance increased rapidly thereafter. In the liquid phase indicated by β, the resistance was linear. The linearity continued until the onset of vaporization at γ. From label γ to δ, the resistance approached a nearly constant value. Within this range, we assumed that the wire changed its form from a liquid to a vapor.

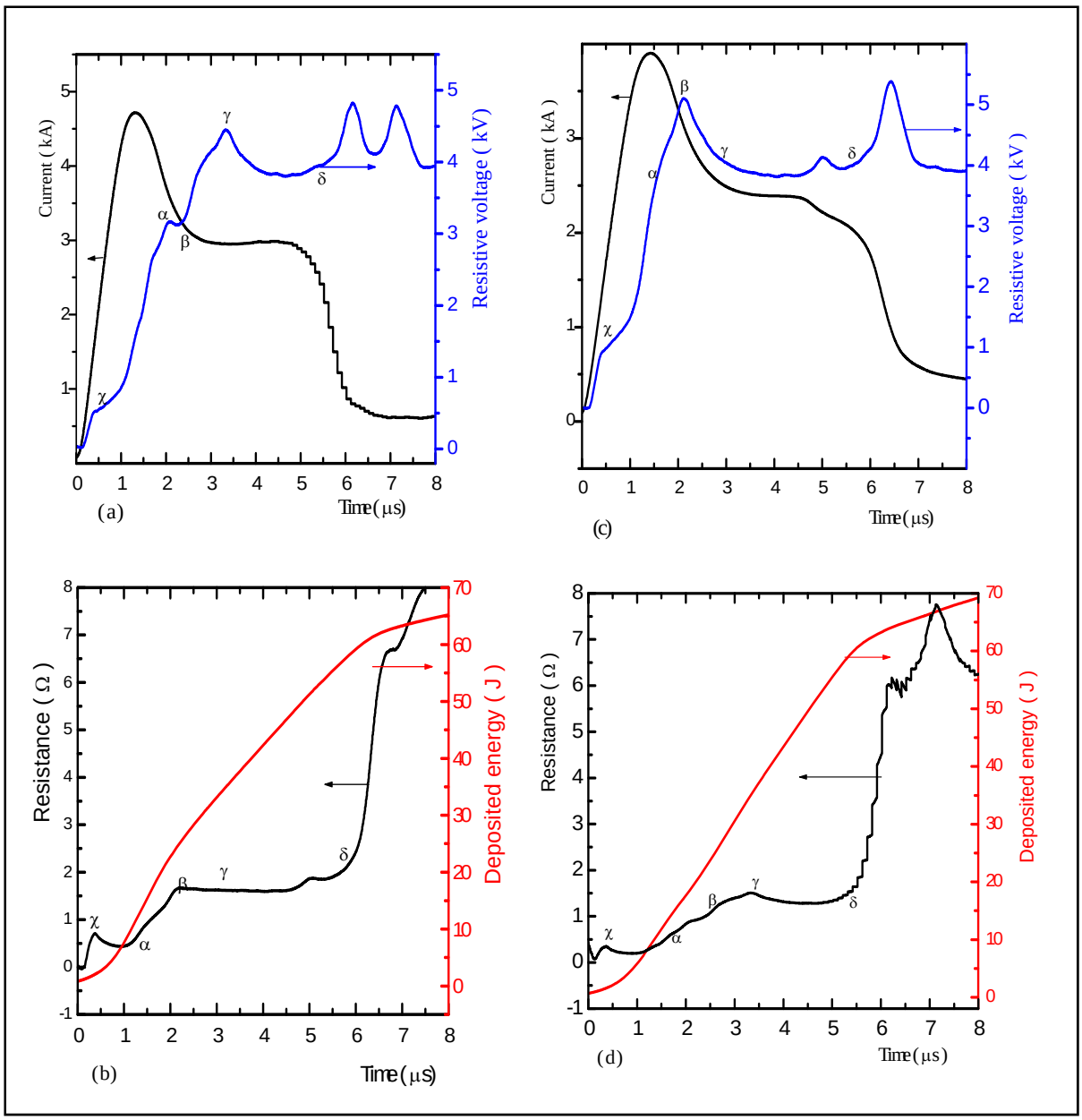

Figure 2. Time record shot of current (dark), voltage (blue), and deposited energy (red) and the resistance (dark) of 230-μm diameter nickel wire exploded in air (a, b) and water (c, d). χ = Curie phase transition, α = onset of melting, β = liquid phase, γ = onset of vaporization, and δ = onset of arcing.

Our measurement (see figure 2b) of $R(t)$ was in excellent agreement with the earlier results in Tkachenko et al. (*12*) and Rousskikh et al. (*13*). It was reported that the resistivity during the liquid phase, expressed as $\rho(t) = \dfrac{V(t)\pi a^2}{I(t)l}$ (where a is radius of the wire and l is the length), varied only slightly over time (*12–14*). Taking our experimental parameters, a =115 μm, l = 0.054 m, and $\dfrac{V(t)}{I(t)}$ = 1.5 Ω, the resistivity at melting is ~1.2 μΩ-m. This compares well with

$\rho(t)$ = 1.5 μΩ-m reported in Tkachenko et al. (*12*), considering that the experimental conditions (such as wire purity) were not provided.

In water, the plot of current, voltage, resistance, and deposited energy is shown in figures 2c and d. The characteristic features of wires exploded in water (see figures 2c and d) are similar to those of wires exploded in air (see figures 2a and b), except that more energy was deposited into wire in water. At χ, ~3.9 J of energy was deposited in water compared to 2.6 J of energy in air. The voltage increased until the deposited energy reached approximately 19 J at α (see figure 2c). By contrast, in air, ~15 J of energy was deposited at α. At β, 25 J of energy was deposited compared to 21 J of energy in air. At γ, 35 J of energy was deposited compared to 30 J in air. Furthermore, at δ, approximately 57 J of energy was deposited in water compared to 52 J in air.

In all the regimes (χ, α, β, γ, and δ) discussed, one recognizes some typical stages. The first stage is the phase transition at χ, followed by heating of the wire and onset of melting at α, melting at β, onset of vaporization at γ, and arcing at δ. We have found that the characteristic current and voltage waveforms are similar in air and water. The energy required to melt a 54-mm-long, 230-μm-diameter nickel wire was estimated to be 18.5 J. The energy required to fully vaporize this wire was 164.5 J. The measured energy deposited up to vaporization was about 52 J in air and 60 J in water, which is ~32% and 36% of the vaporization energy. This finding is consistent with the previous work of Sinars et al. (*15*), who showed that the deposited energy at vaporization was 30% for Al, 55% for Cu, 17% for Pt, 49% for Au, 24% for Fe, 13% for W, and 3% for Ti. They reported that the deposited energy at vaporization depended on the expansion of the exploding wire core. The most rapid and uniform expansion occurred for wires in which the initial energy deposited was a substantial fraction of the energy required to completely vaporize the wire.

4.2 Tungsten

Figure 3 depicts waveforms showing the electrical characteristics of an exploding 150-μm-diameter tungsten wire in air and water. As before, figures 3a–d show the current through the wire, the voltage across the wire, the resistance, and deposited energy. In air (see figure 3a), during the wire heating stage prior to the point χ, the current and voltage linearly increased in time. The current reached a maximum value of about 4.2 kA in 0.75 μs and then dropped to 1.5 kA at 1.5 μs. Similarly, in water (see figure 3c) the current reached a maximum value of 4.4 kA at 0.75 μs and then followed the same pattern as in air.

Meanwhile, the voltage rose from 0 to a maximum value of about 5.9 kV in air and 5.0 kV in water, with inflection at label χ. The label at χ manifested by a local maximum in the resistance of the wire is shown in figure 3b. The initial rise in resistance was previously reported by Tkachenko et al. (*12*) and Rousskikh et al. (*13*) for W wires exploded in air in a nanosecond time

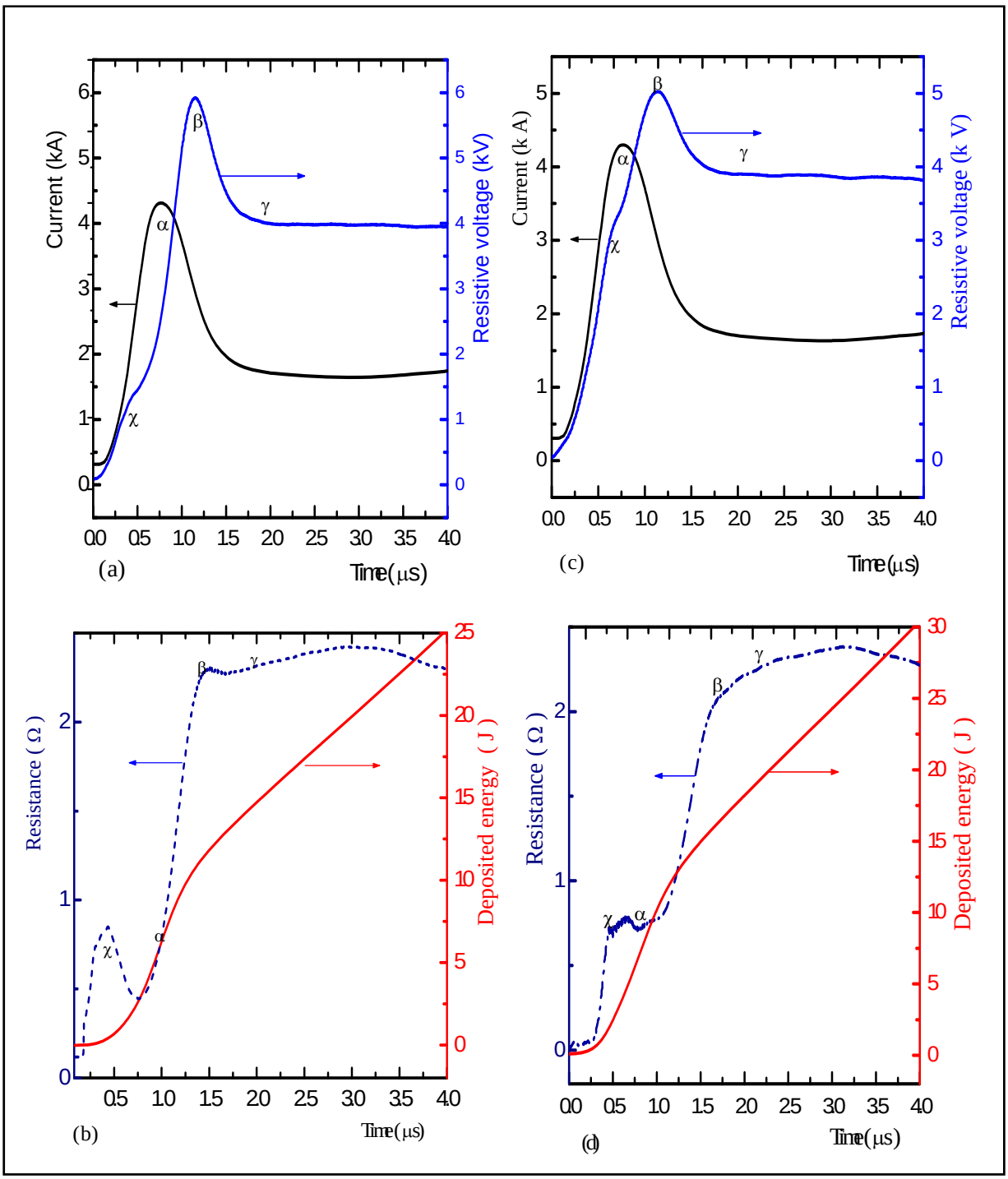

Figure 3. Time record shot of current (dark), voltage (blue), and deposited energy (red) and resistance (dashed) of 150-μm diameter tungsten wire exploded in air (a, b) and water (c, d). χ = fluctuation in heating, α = onset of melting, β = liquid phase, and γ = onset of vaporization.

scale. In Tkachenko et al. (*12*), the time variation of the resistance showed that the local maximum occurred at ~500 ns, similar to our observation (see figure 3b). Meanwhile, in Rousskikh et al. (*13*), the resistance was plotted against deposited energy, showing the local maximum at about 2 mJ. No explanation was given for the initial local maximum of the resistance for W wire exploded in air.

At α (onset of melting), ~6 J of energy was deposited in air, and about 8 J of energy was deposited in water (see figures 2a and c). The deposited energy at α was ~75% (in air) and 98% (in water) of the energy required to raise the temperature of the tungsten wire to the melting point. The energy required to completely melt a 54-mm-long, 150-μm-diameter tungsten wire was estimated to be 11.5 J (see table 1). The measured deposited energy at β was 13 J in air and 15 J in water; these values were sufficient to melt the tungsten wire. As more energy was added into the wire, the wire started to vaporize. At γ, ~18 J of energy was deposited in air and 23 J in water. The deposited energy at γ was sufficient to bring the wire to vaporization point (see table 1).

The resistance for the wire exploded in air and water is shown in figures 3b and d. In both cases, the resistance rose slowly (with various changes in slope) to a maximum value of about 2.25 Ω. The difference in the resistance curves in air and water was attributed to the nonuniformity of the liquid wire in air, i.e., during ohmic heating, rapid expansion usually led to nonuniform densities, and if conditions were nonuniform, conductivity would also be nonuniform. In air, we postulated that at the onset of current pulse, current flowed in a small cross-sectional area of the wire, resulting in increased average wire, resistance (V_R / I) than expected if the current was uniformly distributed in a cross-sectional area of the wire. As the wire was heated, the conducting area grew, forcing the resistance wire to fall to a minimum value (see point α in figures 3b and d). At this point, the specific conductivity decreased, causing the resistance to increase again at label α.

5. Conclusion

An attempt was made to provide a full qualitative description of exploding nickel and tungsten wires in air and water. The primary measurements were the current through and voltage along the plasma column. Using these data as input, we then deduced the resistance and deposited energy in the plasma. A comparison of the experimental results for the explosion of nickel and tungsten wires in air with the results for the explosion in water showed that more energy was deposited in water than in air. We postulated that water prevented rapid expansion of the heated wire, enabling the material to be uniform during explosion and improving energy deposition. The mechanism causing the increase in energy deposition is still not well understood. We

postulated that plasma formation outside the wire core (in air explosion) was responsible for the reduction in deposited energy.

Finally, the experiments presented in this report, along with ongoing and future experiments, should ultimately prove useful for determining appropriate wire thermodynamic properties at high temperatures and pressures. This could occur through trial and error with some materials or by helping to validate computer codes, such as ALEGRA, that can then be used to predict the results of changing wire materials.

6. References

1. Sarkisvo, G. S.; Bauer, B. S.; De Groot, J. S. Homogeneous Electrical Explosion of Tungsten Wire in Vacuum. *Journal of Theoretical Physics Letters* **2001**, *73*, 74–79.

2. Sarkisov, G. S.; Rosenthal, S. E.; Cochrane, K.; Struve, K. W.; Deeney, C.; McDaniel, D. H. Nanosecond Electrical Explosion of Thin Copper Wires in a Vacuum: Experimental and Computational Investigations. *Physics Review Letter, E 71* **2005**, 46404.

3. Sarkisov, G. S.; Struve, K. W.; McDaniel, D. H. Effect of Deposited Energy on the Structure of an Exploding Tungsten Wire Core in a Vacuum. *Physics of Plasmas* **2005**, *12* (5), 052702.

4. Grinenko, E.; Krasik, Ya. E.; Efimov, S.; Fedotov, A.; Gurovich, V. Nanosecond Time Scale High Power Electrical Wire Explosion in Water. *Physics of Plasmas* **2006**, *13*, 42701.

5. Bennett, F. D. In *Progress in High Temperature Physics and Chemistry*; Rouse, C. A., Ed.; Pergamon: Oxford, 1968; vol. 2, p. 3.

6. DeSilva, A. W.; Kunze, H. J. Experimental Study of the Electrical Conductivity of Strongly Coupled Copper Plasmas. *Physics Review E* **1994**, *49*, 4448–4454.

7. DeSilva, A. W.; Katsouros, J. D. Electrical Conductivity of Dense Copper and Copper Plasmas. *Physics Review E* **1998**, *5*, 5945.

8. Brauer, J. R. Magnetic Diffusion Times for Infusion and Effusion in Nonlinear Steel Slabs and Cylinders. *IEEE Transactions on Magnetics* **2007**, *43* (7).

9. Cezairliyan, A.; Miiller, A. P. Heat Capacity and Electrical Resistivity of Nickel in the Range 1300–1700 K Measured With a Pulse Heating Technique. *International Journal of Thermophysics* **1983**, 389–396.

10. *Handbook of Chemistry and Physics*; 44th ed.; Lide, D. R., Ed.; Chemical Rubber Publishing Co.: Cleveland, OH, 1962.

11. White, G. K.; Minges, M. L. *Thermophysical Properties of Some Key Solids*; CODATA Bulletin No. 59; Pergamon: Oxford, 1985.

12. Tkachenko, S. I.; Pikuz, S. A.; Romanova, V. M.; Ter-Oganesyan, A. E.; Mingaleev, A. R.; Shelkovvenko, T. A. Overvoltage Pulse Development Upon Electrical Explosion of Thin Wires. *J. Phys. D: Appl. Phys*. **2007**, *40*, 1742–1750.

13. Rousskikh, A. G.; Oreshkin, V. I.; Labetsky, A. Yu.; Chaikovsky, S. A.; Shishlov, A. V. Electrical Explosion of Conductors in the High-Pressure Zone of a Convergent Shock Wave. *Technical Physics* **2007**, *52* (5), 571–576.

14. Rakhel, A. D.; Kloss, A.; Hess, H. On the Critical Point of Tungsten. *International Journal of Thermophysics* **2002**, *23* (5).

15. Sinars, D. B.; Min Hu, K.; Chandler, M.; Shelkovenko, T. A.; Pikuz, S. A.; Greenly, J. B.; Hammer, D. A.; Kusse, B. R. Experiments Measuring the Initial Energy Deposition, Expansion Rates and Morphology of Exploding Wires With About 1 kA/Wire. *Physics of Plasmas* **2001**, *8* (1), 19–33.

NO. OF COPIES	ORGANIZATION
1 (PDF only)	DEFENSE TECHNICAL INFORMATION CTR DTIC OCA 8725 JOHN J KINGMAN RD STE 0944 FORT BELVOIR VA 22060-6218
1	DIRECTOR US ARMY RESEARCH LAB IMNE ALC HR 2800 POWDER MILL RD ADELPHI MD 20783-1197
1	DIRECTOR US ARMY RESEARCH LAB AMSRD ARL CI OK TL 2800 POWDER MILL RD ADELPHI MD 20783-1197
1	DIRECTOR US ARMY RESEARCH LAB AMSRD ARL CI OK PE 2800 POWDER MILL RD ADELPHI MD 20783-1197
	ABERDEEN PROVING GROUND
1	DIR USARL AMSRD ARL CI OK TP (BLDG 4600)

NO. OF
COPIES ORGANIZATION

ABERDEEN PROVING GROUND

18 DIR USARL
AMSRD ARL WM
J FLENIKEN
AMSRD ARL WM TA
B DONEY
M KORNECKI
S SCHOENFELD
J RUNYEON
AMSRD ARL WM TE
P BERNING
C HUMMER
T KOTTKE
M MCNEIR
A NIILER
J POWELL
B RINGERS
G THOMSON
U UHLIG
G VUNNI (4 CPS)